Nonlinear viscoelasticity of adherent cells is controlled by cytoskeletal tension†

Philip Kollmannsberger,* **Claudia Tanja Mierke and Ben Fabry**

The viscoelastic response of living cells to small external forces and deformations is characterized by a weak power law in time. The elastic modulus of cells and the power law exponent with which the elastic stresses decay depend on the active contractile prestress in the cytoskeleton. It is unknown whether this also holds in the physiologically relevant regime of large external forces and deformations. We used magnetic tweezers to apply stepwise increasing forces to magnetic beads bound to the cytoskeleton of different cell lines, and recorded the resulting cell deformation (creep response). The creep response followed a weak power law at all force levels. Stiffness and power law exponent increased with force in all cells, indicating simultaneous stress stiffening and fluidization of the cytoskeleton. The amount of stress stiffening and fluidization differed greatly between cell types but scaled with the contractile prestress as the only free parameter. Our results demonstrate that by modulating the internal mechanical tension, cells can actively control their mechanical properties over an exceedingly large range. This behavior is of fundamental importance for protection against damage caused by large external forces, and allows the cells to adapt to the highly variable and nonlinear mechanical properties of the extracellular matrix.

Introduction

Living cells are very soft, with elastic moduli typically on the order of one kilo-Pascal. To form larger multicellular organisms, the mechanical support provided by connective tissue and skeletal structures is therefore essential. The mechanical properties of the cells are nonetheless important for a number of functions such as cell division, phagocytosis, migration, and contraction. Living cells form a complex active material with both solid-like elastic and fluid-like viscous properties. In response to external mechanical stress, they exhibit viscoelastic phenomena such as creep and stress relaxation. A striking feature is that the viscoelastic moduli show a weak power-law dependence on time or frequency, corresponding to the absence of any characteristic relaxation times in the system.[1–6] The two parameters of this power law, stiffness and power law exponent, are not independent: stiff cells in general have a smaller power law exponent and thus appear more solid-like than soft cells.[4]

The power law rheology of living cells is linked to another important mechanical property: the active internal tension generated by the actomyosin cytoskeleton. The stiffness of adherent cells increases linearly with their contractile tension.[7] Consequently, the three parameters stiffness, power law

exponent, and contractile tension are linked by a simple phenomenological relationship. These observations are universal and hold independent of cell type and experimental technique[8,9] as long as measurements are carried out using small forces and deformations to ensure a force-independent linear response. However, the large forces and deformations that cells experience under physiological conditions in the living organism often exceed the linear regime.[10]

Measurements of cell mechanical properties have also been carried out in a high-force or large-deformation regime, but with contradictory results. Cells have been reported to stiffen,[11–13] to fluidize and yield,[14,15] or to remain completely linear and time-scale invariant[3] after application of external stretch, depending on experimental conditions and cell models used. Single cell measurements in the non-linear regime are technically difficult, however, and in particular the separation between non-linear elastic and non-linear viscous responses is challenging.

For this study, we developed a technique that allowed us to measure the time- and force-dependent viscoelastic properties of adherent cells in response to large forces.[16] The microrheological creep response of seven different cell types was determined by applying a staircase-like sequence of increasing force steps to magnetic beads bound to the cytoskeleton. The resulting bead displacements were recorded and analyzed using a force-dependent superposition approach to distinguish between time-dependent and force-dependent properties. We found power-law time dependence of the creep response regardless of the applied force, and an increase of both the stiffness and the power law

Center for Medical Physics and Technology, Henkestr. 91, 91052 Erlangen, Germany. E-mail: pkollmannsberger@biomed.uni-erlangen.de; Fax: +49-9131-8525601; Tel: +49-9131-8525610

exponent with force, indicating simultaneous stress stiffening and fluidization. Stiff and elastic cells stiffen less but fluidize more compared to soft and fluid-like cells. Stiffness data from all cell types and all force levels were found to depend only on the sum of cytoskeletal prestress and externally applied stress, *i.e.* the total mechanical tension in the cell. The increase of the power law exponent with increasing external stress was also found to depend on cytoskeletal prestress, consistent with the notion of force-dependent unbinding of elastic cytoskeletal bonds as the main source of stress dissipation.

Our results show that living cells can actively tune their stress stiffening and fluidization behavior in response to large external forces by modulating their cytoskeletal prestress. To adapt to different mechanical conditions, cells need to adjust only the activity of their actomyosin contractile apparatus. The cytoskeletal prestress defines the constitutive elastic and frictional behaviors both in the linear and non-linear regime, for a variety of cytoskeletal manipulations, for a wide range of timescales, and for diverse cell types. Our finding may be important for a quantitative description of biological processes involving a mechanical interaction between cells and their environment, such as matrix remodeling, mechanosensing, or tissue development.

Results

Power law behavior holds at all forces

When a constant force pulse f_0 was applied to magnetic beads bound to integrin cell surface receptors, the resulting bead displacement $d(t)$ always followed a weak power law, $d(t) \propto t^\beta$. This power-law time dependence was independent of the applied force magnitude (Fig. 1). We estimate the typical strain $\gamma(t)$ as the displacement $d(t)$ divided by the bead radius r, and the typical stress σ as the applied force divided by the bead cross-sectional area, $r^2\pi$. The creep compliance $J(t)$ in units of Pa^{-1} is then given by $d(t)/f$ times a constant geometric factor $\pi r \approx 7.1$ μm and is fit to the equation

$$J(t) = J_0(t/t_0)^\beta \qquad (1)$$

with time normalized to $t_0 = 1$ s. The power-law exponent β characterizes the time-dependent viscoelastic properties and was between 0.1 and 0.5, where $\beta = 0$ corresponds to an elastic solid and $\beta = 1$ to a viscous fluid. The inverse of the prefactor, $1/J_0$, is equivalent to a shear modulus K_0 at time $t = 1$ s. J_0 decreased with force (Fig. 1c), indicating stress stiffening and the breakdown of linear superposition. With this protocol, however, a cell cannot be measured repeatedly at multiple force levels because the cytoskeletal structure may not return quickly enough to its undisturbed state in between measurements, and also because at longer timescales cells can actively respond to force. With only one force level per cell, the force dependence might be confounded by the large cell-to-cell variability of the mechanical properties. Moreover, a single force step can only measure the secant moduli that are less sensitive to force compared to a differential measurement. From single-step creep experiments, therefore, no reliable conclusion about the force dependence can be made.
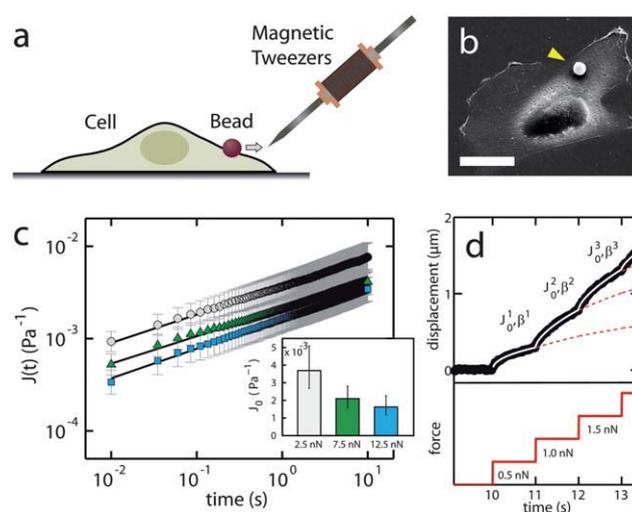
Fig. 1 Fig. 1Measurement of nonlinear viscoelastic properties of adherent cells using magnetic microrheology and a differential creep protocol. (a) The gradient force generated by magnetic tweezers acts on superparamagnetic beads coated with fibronectin that are bound to the cytoskeleton of adherent cells *via* integrin receptors. (b) SEM image of a fibroblast with a 4.5 μm bead (arrow) bound to its surface. Scale bar = 20 μm. (c) Creep response to force steps of 2.5 nN (top), 7.5 nN (middle) and 12.5 nN (bottom) always followed a power law over time, $J(t) = J_0(t/t_0)^\beta$. Inset: the decrease of the prefactor J_0 with increasing force indicates stress stiffening. (d) A staircase-like sequence of increasing force steps was applied, and the displacement was fit to a superposition of creep processes (eqn (5) and (6)).

Stress stiffening

In order to quantify the force dependence of the creep response and the parameters J_0 and β, a staircase-like sequence of increasing force steps was applied in a single measurement. The displacement after the nth force step at time t_n was fitted to a superposition of creep processes with a response function $J(t)$ that depends not only on time but also on the currently applied total force (see Materials and methods). Stress stiffening (increase of $1/J_0$ with force) as well as fluidization (increase of β with force) were observed in all cell types. Fibroblasts were on average 3.5 fold stiffer but showed less stress stiffening compared to epithelial cells. To quantify the relationship between stiffness and stress stiffening, data from all experiments were pooled and grouped by stiffness. The stiffest and most elastic cells showed the smallest amount of stress stiffening (Fig. 2).

In the following, we show that different degrees of stiffening are caused by different levels of prestress in the cell. We take the total mechanical tension in the cytoskeleton as the sum of active (myosin-generated) internal prestress σ_p and passive external stress σ_e imposed by the magnetic bead. This mechanical tension is counterbalanced by the substrate so that all internal and external forces sum up to zero. Furthermore, we assume that the linear relationship between the differential stiffness K' and the cytoskeletal stress, which has been previously reported for various cell types[7,11,17] is a universal property and also holds in the cell lines tested here. K' can then be expressed as

$$K'(\sigma) = \frac{d\sigma}{d\gamma} = K_0' + a(\sigma_p + \sigma_e) \qquad (2)$$
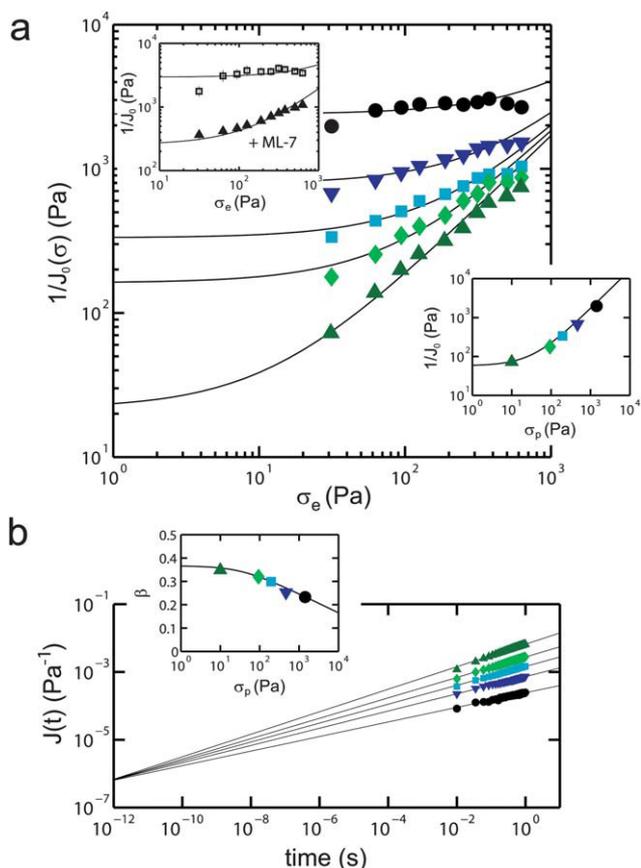
Fig. 2 The stress stiffening follows a simple relationship with the total cytoskeletal mechanical stress. (a) Stiffness $1/J_0$ *versus* applied stress, grouped by the stiffness at the smallest force ($n = 395$ cells). Stiff cells show less stress stiffening compared to soft cells. Black lines: fit of eqn (2) with common parameters $a = 1.68$ and $K_0' = 5$ Pa, and prestress as free parameter. (Top inset) Inhibition of cytoskeletal prestress by ML-7 in MEF cells (black triangles) reduced stiffness and accentuated stress stiffening compared to untreated cells (open squares). (Lower inset) Initial stiffness $1/J_0$ *vs.* prestress for all data. Solid line: prediction by eqn (2). (b) Creep response $J(t)$ for the first force step *vs.* time, same grouping as in (a). Solid lines: fit to eqn (3), with common parameters $j_0 = 5.59 \times 10^{-7}$ Pa^{-1} and $\tau_0 = 5.5 \times 10^{-13}$ s, and β as free parameter. (Inset) Measured exponent *vs.* prestress from (a). Solid line: prediction from eqn (4). Standard errors are smaller than symbol size in all cases.

where the prefactor a characterizes the dependence of stiffness on stress, and K_0' denotes the linear stiffness at the force-free state.

We could fit eqn (2) to all force–stiffness curves in Fig. 2a using only a single value for K_0' and a, leaving the contractile prestress σ_p as the only free parameter. This implies not only that cells with higher prestress are stiffer but also that the relative increase of total mechanical tension due to external forces is smaller and therefore causes only small additional stress stiffening. The values of prestress obtained from the fit of eqn (2) are proportional to the average measured stiffness at the smallest force (Fig. 2, inset). The validity of eqn (2) is supported by additional observations: first, the fit yields prestress values of up to 1500 Pa, which is on the order of the maximum traction stress that adherent cells can exert on their substrate.[7] Second, the values for the linear modulus K_0' in the absence of prestress are in the range of a few Pa, which is similar to the stiffness of unstressed

crosslinked actin networks.[18] And third, integration of eqn (2) yields an exponential stress–strain relationship, which is characteristic of many biological tissues[10] and has also been observed when stretching whole cells.[11] The quality of the fit can only be marginally improved with a non-linear stiffness–prestress relationship according to $K'(\sigma) = K_0' + a\sigma^x$. The fitted value of the exponent x is 1.13, which is close to unity and therefore in support of a linear stiffness–prestress relationship.

Ruling out active cell responses

We performed a number of tests to rule out that the observed stress stiffening after force application is a result of mechano-chemical signal transduction processes. First, we suppressed actomyosin contraction with the myosin light chain kinase (MLCK) inhibitor ML-7[19] in the highly contractile mouse embryonal fibroblast (MEF) cells. As predicted by eqn (2), a reduction of prestress by ML-7 results in reduced stiffness and more pronounced passive stress stiffening (Fig. 2, inset). Force-induced contraction therefore cannot explain the observed stress stiffening. Second, we used beads coated with poly-L-lysine instead of fibronectin. Such beads connect to the cytoskeleton through membrane-associated proteins without inducing integrin activation or focal adhesion reinforcements,[20,21] and force application to such beads does not induce mechano-sensitive active responses.[22] The resulting stress stiffening response, however, is indistinguishable from that obtained with FN-coated beads (Fig. S1†). The influence of other mechano-transduction mechanisms such as cell contraction in response to stretch-activated ion channel activation can be ruled out by the fact that the stiffening response was instantaneous (Fig. 1c), and the power-law slope of the creep-response was constant at all timescales (Fig. 2b). To exclude stiffening due to active remodeling of the cytoskeleton on longer timescales, we completed our experiments within ten seconds.

Power law rheology and stiffening

More contractile cells are not only stiffer, they also display a smaller power law exponent and hence more solid-like properties compared to less contractile cells.[4,23] In particular, the creep response curves from differently contractile cells, when extrapolated to short timescales, pivot around a common intersection, or fixed point j_0, at very small time τ_0 of 10^{-11} s to 10^{-15} s,[5] and obey the scaling equation

$$J(t) = j_0(t/\tau_0)^\beta \tag{3}$$

with $\beta > 0$. We validated this observation in our data by fitting the creep response during the first force step (500 pN) to eqn (3) with a common intersection at $j_0 = 5.59 \times 10^{-7}$ Pa^{-1} and $\tau_0 = 5.5 \times 10^{-13}$ s (Fig. 2a, inset). For eqn (2) and (3) to hold at the same time in the linear regime (the external stress σ_e is small compared to the prestress σ_p), the following relationship between prestress, stiffness and power law exponent must also hold:[23]

$$\beta(\sigma_p) = \frac{\ln\left[j_0\left(K_0' + a\sigma_p\right)\right]}{\ln(\tau_0/1s)} \tag{4}$$

Indeed, the creep exponent obtained from the data in Fig. 2b, when plotted against the prestress obtained from the data in

Fig. 2a, closely follows eqn (4) without any further adjustment of parameters (Fig. 2b, inset). Consequently, the response of living cells to large external forces is described by a single relationship which links power law rheology to nonlinear elasticity. The only free parameter that defines this relationship is the contractile cytoskeletal prestress σ_p.

Fluidization

The power law exponent β increased in all cells with the logarithm of the external force, indicating force-induced fluidization and yielding events (Fig. 3). We define fluidization here as an increase of the power law exponent, regardless of concurrent stiffness changes. We find, surprisingly, that fluidization and stress stiffening occur at the same time in the same cell.

The amount of fluidization with external force differed between cells and was quantified by the slope $z = \mathrm{d}\beta/\mathrm{d}(\log \sigma_e)$. Cells with more solid-like behavior (small β) showed the most pronounced fluidization (largest z), whereas cells that were initially more fluid-like (large β) showed no further increase of β during creep (small z). The fluidization slope z decreased linearly with increasing β (Fig. 3, bottom inset), which in turn depends on cytoskeletal prestress σ_p according to eqn (4). Therefore, the fluidization of cells in response to large external forces is modulated mainly by the prestress. In agreement with this observation, we found attenuated fluidization responses in MEF cells after the actomyosin contraction was suppressed with the MLCK inhibitor ML-7 (Fig. 3, top inset).

Discussion

Power law rheology, stress stiffening and fluidization in adherent cells have been reported in numerous studies using diverse experimental methods. The present study shows that these three
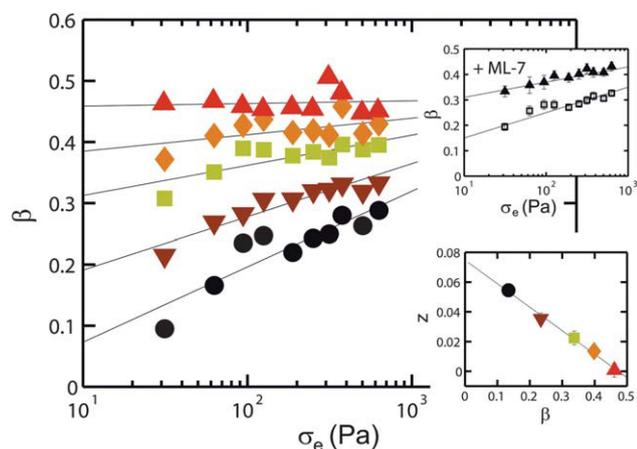
Fig. 3 The power law exponent increases with applied external stress. Data for all cell lines are grouped by the exponent at the smallest force ($n = 395$). Elastic cells (small β) show a higher amount of fluidization in response to force application compared to more fluid cells (large β). (Top inset) Inhibition of cytoskeletal prestress by ML-7 in MEF cells (black triangles) leads to an increase in β but reduces fluidization compared to untreated cells (open squares). (Lower inset) The amount of fluidization, or slope of the solid black lines, z, decreases linearly with the initial exponent. Standard errors are smaller than symbol size in all cases.

phenomena are not independent of each other, but are linked by a single common parameter, which is the cellular prestress. This discovery, together with previous findings on the universality of cell mechanical behavior, strongly indicates a common underlying structural origin for power law rheology, stress stiffening and fluidization.[9] However, a constitutive theory of cell mechanics from which the phenomenological relationship reported here could be derived has not been developed so far. Instead, a number of different theoretical explanations exist that each captures different aspects of cell mechanical behavior.

Passive stress stiffening is a generic property in biopolymer networks, cells, and tissues. There are various mechanisms that account for passive stiffening. In fibrous materials, alignment of initially sloppy fibers along the direction of deformation causes an increased resistance or stress.[10] On a microscopic level, the nonlinear force–elongation relationship of individual semiflexible filaments contributes to the stress stiffening behavior of the network.[24–26] The linear relationship between stiffness and external stress that we and others report[11,24] corresponds to the exponential stress–strain relationship that is characteristic of many biological materials.[10]

In adherent cells, stress stiffening occurs not only due to external stress, but also in response to internally generated contractile forces that are counterbalanced by stiff microtubules or by the substrate the cell adheres to.[7] In this regard, cells behave like tensegrity structures.[7,27] Simple tensegrity models with few elements can quantitatively explain the linear relationship between differential stiffness and cellular prestress.[28] In principle, such models can be extended to describe power law rheology by incorporating viscoelastic elements[29] or structural rearrangements[30] into prestressed tensegrity structures. The importance of prestress for power law rheology in tensegrity structures is debated, however. Suspended cells, which cannot develop prestress against a substrate, seem to exhibit a different behavior,[31] although a recent study reports power law rheology also in suspended cells.[32]

Timescale-free power-law behavior indicates a broad distribution of relaxation times of the underlying microscopic dissipation mechanism, as described by the theory of Soft Glassy Rheology (SGR).[33] SGR theory has been a useful concept for understanding cell mechanical behavior and has generated a large number of predictions that have been experimentally confirmed,[14,15] supporting the analogy between living cells and soft glassy materials. While SGR is in good agreement with the power-law behavior and stress-induced fluidization that we report here, it does not account for stress stiffening.

This limitation has recently been overcome by combining the SGR concept with the wormlike chain (WLC) description of semiflexible polymers to explain stiffening, fluidization and power law rheology in a single model.[34–36] The Glassy Wormlike Chain (GWLC) model describes the retardation of filament relaxation due to sticky interactions, leading to an exponential stretching of the $\omega^{3/4}$ relaxation spectrum of individual filaments. The idea behind this concept is generic and applicable to cells and other heterogeneous biological materials. There is experimental evidence that at least in the high-frequency regime, cells show a $\omega^{3/4}$ scaling as predicted by the wormlike chain model.[8,37] Semiflexible polymer models can also account for the decrease of the power law exponent with increasing prestress because the

propagation of free energy along the filament depends on the prestress.[38]

Rigidly crosslinked semiflexible polymer networks exhibit a stiffening exponent of 1.5 with stress,[39] which is in accordance with WLC models but different from the linear relationship we observe. Networks with more compliant crosslinkers such as filamin, however, exhibit a linear dependence of stiffness on stress, and they show a decrease in the power law exponent with increasing stress.[40–42] This behaviour is strikingly similar to the behaviour of living cells and points towards a prominent role of the elasticity and dynamics of crosslinks for the nonlinear mechanical properties of cells.[18] Due to the structural complexity of the cytoskeleton, however, a single crosslinker alone such as filamin cannot account for the nonlinear rheological properties of the cell.[43] Instead, the fact that stress stiffening, power-law rheology and fluidization are observed in a wide variety of biological and biopolymer systems of different molecular compositions but similar structural architecture leads to the conclusion that the common rheological features have no specific molecular but rather a structural origin, such as dynamic bond turnover or tensegrity.

On a molecular level, the mechanism of contractile force generation is the interaction of actin and myosin filaments, which is well captured by the sliding filament model of skeletal muscle proposed by Huxley[44] and Huxley and Simmons.[45] The Huxley model resembles the SGR model in that it contains multiple binding interaction energies, but with the addition of a force-generating mechanism based on a Brownian ratchet. Highly contractile cells such as fibroblasts and myoblasts exhibit a remarkably muscle-like mechanical phenotype.[12,46] Conversely, smooth muscle tissue also shows cell-like power law rheology, stretch-induced fluidization and a reduced power law exponent with increasing contractile activation.[4,47] The latter is thought to reflect a reduced actomyosin cycling rate due to a strongly bound state of actin and myosin under contraction.[48,49] From this perspective, a combination of soft glassy rheology and models of muscle contraction appears to be a promising approach towards describing cell mechanics.[50]

Summary

Our results demonstrate that adherent cells control the amount of stress stiffening and fluidization in response to large external forces by modulating their contractile prestress. Highly contractile cells are not only stiffer and more solid-like, they also show less stress stiffening and increased fluidization compared to less contractile cells.

The biological relevance of such nonlinear viscoelastic behavior is wide-ranging. Soft and liquid-like cells, on the one hand, need to stiffen in order to withstand large mechanical stress. Stiff and solid-like cells, on the other hand, depend on fluidization in order to be able to withstand large mechanical strain without rupturing. Thus, by a single mechanism that is present in all eukaryotic cell types—namely, by modulating the activity of actomyosin contraction—cells can adapt to a wide range of mechanical conditions. Moreover, by modulating their contractile prestress, cells also change the mechanical state of their environment, which is again sensed by the cells.[51,52] This mechanical feedback loop may be essential for the control and robustness of many developmental growth processes. In this connection, it is interesting that the passive nonlinear viscoelasticity of cells closely resembles that of the extracellular matrix.[10]

Our data show that the time-dependent mechanical responses of adherent cells to large forces and deformations obey clearly defined empirical laws. Their knowledge is important for a quantitative understanding of biological processes involving mechanical interaction between cells and their environment, such as matrix remodeling, mechanosensing, cell migration or tissue development.

Materials and methods

Cell culture

Mouse embryonal fibroblasts (MEFs), NIH 3T3 mouse fibroblasts, F9 mouse embryonic carcinoma cells, MeWo human fibroblast-like cells, and MDA-MB231, 786-O and A125 human epithelial cancer cells were maintained in Dulbecco's modified Eagle's medium supplemented with 10% fetal calf serum (low endotoxin), 2 mM L-glutamine, and 100 U mL^{-1} penicillin/streptomycin (Dulbecco's modified Eagle's medium, complete medium; Biochrom, Berlin, Germany) and kept at 37 °C with 5% CO_2. One day prior to measurements, cells were harvested at 80% confluence, seeded in 35 mm culture dishes (Nunclon Surface, Nunc, Wiesbaden, Germany) at a density of 2×10^5 cells, and maintained at 37 °C and 5% CO_2 overnight.

Magnetic tweezer experiments

To measure the creep response, we used a magnetic tweezer setup that was optimized for applying high forces in the 10 nN range to magnetic beads bound to living cells[16] (Fig. 1a). A single force step or a staircase-like increasing force was applied for 10 seconds. The resulting bead displacement $d(t)$ was determined from images recorded with a CCD-camera (Orca-ER, Hamamatsu) at a rate of 40 frames s^{-1}. Details of the experimental protocol are described in ref. 53.

Data analysis

In the case of linear viscoelasticity, the creep response to a force staircase is a superposition of power laws with identical parameters but different starting times. For single-step creep experiments we have shown that the power law fit remains applicable regardless of the force level (Fig. 1c). The parameters, however, change with force, revealing that cells are a nonlinear viscoelastic material[11] and the superposition approach fails. Instead of a single elastic modulus G', nonlinear elasticity can be quantified using a differential stiffness K', which is defined as the slope of the stress–strain curve.[10,26] Accordingly, we model the response to each individual force step by a differential creep response

$$\gamma(t \geq t_n) = \gamma(t_n) + \sum_{i=0}^{n} [J_\sigma(t - t_i) - J_\sigma(t_n - t_i)]\sigma_i \quad (5)$$

with a creep response $J_\sigma(t)$ that depends not only on time but also on the total stress:

$$J_\sigma(t) = J_0(\sigma)(t/t_0)^{\beta(\sigma)} \quad (6)$$

The creep compliance $J_0(\sigma)$ corresponds to the inverse of a stress-dependent differential elasticity $K'(\sigma)$, and the power law exponent describes the time dependence of the creep response at each force level. Bead displacement data were analyzed and fit using custom-written MATLAB programs.

Acknowledgements

References

1 J. Alcaraz, L. Buscemi, M. Grabulosa, X. Trepat, B. Fabry, R. Farre and D. Navajas, *Biophys. J.*, 2003, **84**, 2071–2079.
2 M. Balland, N. Desprat, D. Icard, S. Fereol, A. Asnacios, J. Browaeys, S. Henon and F. Gallet, *Phys. Rev. E: Stat., Nonlinear, Soft Matter Phys.*, 2006, **74**, 021911.
3 N. Desprat, A. Richert, J. Simeon and A. Asnacios, *Biophys. J.*, 2005, **88**, 2224–2233.
4 B. Fabry, G. N. Maksym, J. P. Butler, M. Glogauer, D. Navajas and J. J. Fredberg, *Phys. Rev. Lett.*, 2001, **87**, 148102.
5 G. Lenormand, E. Millet, B. Fabry, J. P. Butler and J. J. Fredberg, *J. R. Soc. Interface*, 2004, **1**, 91–97.
6 S. Yamada, D. Wirtz and S. C. Kuo, *Biophys. J.*, 2000, **78**, 1736–1747.
7 N. Wang, K. Naruse, D. Stamenovic, J. J. Fredberg, S. M. Mijailovich, I. M. Tolic-Norrelykke, T. Polte, R. Mannix and D. E. Ingber, *Proc. Natl. Acad. Sci. U. S. A.*, 2001, **98**, 7765–7770.
8 B. D. Hoffman, G. Massiera, K. M. Van Citters and J. C. Crocker, *Proc. Natl. Acad. Sci. U. S. A.*, 2006, **103**, 10259–10264.
9 X. Trepat, G. Lenormand and J. J. Fredberg, *Soft Matter*, 2008, **4**, 1750–1759.
10 Y. C. Fung, *Mechanical Properties of Living Tissues*, Springer-Verlag Inc., New York, 1993.
11 P. Fernandez, P. A. Pullarkat and A. Ott, *Biophys. J.*, 2006, **90**, 3796–3805.
12 D. Mitrossilis, J. Fouchard, A. Guiroy, N. Desprat, N. Rodriguez, B. Fabry and A. Asnacios, *Proc. Natl. Acad. Sci. U. S. A.*, 2009, **106**, 18243–18248.
13 N. Wang, J. P. Butler and D. E. Ingber, *Science*, 1993, **260**, 1124–1127.
14 P. Bursac, G. Lenormand, B. Fabry, M. Oliver, D. A. Weitz, V. Viasnoff, J. P. Butler and J. J. Fredberg, *Nat. Mater.*, 2005, **4**, 557–561.
15 X. Trepat, L. Deng, S. S. An, D. Navajas, D. J. Tschumperlin, W. T. Gerthoffer, J. P. Butler and J. J. Fredberg, *Nature*, 2007, **447**, 592–595.
16 P. Kollmannsberger and B. Fabry, *Rev. Sci. Instrum.*, 2007, **78**, 114301–114306.
17 A. J. Engler, S. Sen, H. L. Sweeney and D. E. Discher, *Cell*, 2006, **126**, 677–689.
18 O. Lieleg, M. M. A. E. Claessens and A. R. Bausch, *Soft Matter*, 2010, **6**, 218–225.
19 M. Saitoh, T. Ishikawa, S. Matsushima, M. Naka and H. Hidaka, *J. Biol. Chem.*, 1987, **262**, 7796–7801.
20 C. Metzner, C. Raupach, C. T. Mierke and B. Fabry, *J. Phys.: Condens. Matter*, 2010, **22**, 194105–194108.
21 D. Riveline, E. Zamir, N. Q. Balaban, U. S. Schwarz, T. Ishizaki, S. Narumiya, Z. Kam, B. Geiger and A. D. Bershadsky, *J. Cell Biol.*, 2001, **153**, 1175–1186.
22 Y. Wang, E. L. Botvinick, Y. Zhao, M. W. Berns, S. Usami, R. Y. Tsien and S. Chien, *Nature*, 2005, **434**, 1040–1045.
23 D. Stamenovic, B. Suki, B. Fabry, N. Wang and J. J. Fredberg, *J. Appl. Physiol.*, 2004, **96**, 1600–1605.
24 M. L. Gardel, F. Nakamura, J. Hartwig, J. C. Crocker, T. P. Stossel and D. A. Weitz, *Phys. Rev. Lett.*, 2006, **96**, 088102.
25 C. Storm, J. J. Pastore, F. C. MacKintosh, T. C. Lubensky and P. A. Janmey, *Nature*, 2005, **435**, 191–194.
26 M. L. Gardel, J. H. Shin, F. C. MacKintosh, L. Mahadevan, P. Matsudaira and D. A. Weitz, *Science*, 2004, **304**, 1301–1305.
27 D. Stamenovic and D. E. Ingber, *Soft Matter*, 2009, **5**, 1137–1145.
28 M. F. Coughlin and D. Stamenovic, *Biophys. J.*, 2003, **84**, 1328–1336.
29 C. Sultan, D. Stamenovic and D. E. Ingber, *Ann. Biomed. Eng.*, 2004, **32**, 520–530.
30 P. Canadas, S. Wendling-Mansuy and D. Isabey, *J. Biomech. Eng.*, 2006, **128**, 487–495.
31 F. Wottawah, S. Schinkinger, B. Lincoln, R. Ananthakrishnan, M. Romeyke, J. Guck and J. Kas, *Phys. Rev. Lett.*, 2005, **94**, 098103.
32 J. M. Maloney, D. Nikova, F. Lautenschlager, E. Clarke, R. Langer, J. Guck and K. J. Van Vliet, *Biophys. J.*, 2010, **99**, 2479–2487.
33 P. Sollich, F. Lequeux, P. Hébraud and M. E. Cates, *Phys. Rev. Lett.*, 1997, **78**, 2020–2023.
34 C. Semmrich, T. Storz, J. Glaser, R. Merkel, A. R. Bausch and K. Kroy, *Proc. Natl. Acad. Sci. U. S. A.*, 2007, **104**, 20199–20203.
35 L. Wolff, P. Fernandez and K. Kroy, *New J. Phys.*, 2010, **12**, 1–18.
36 K. Kroy, *Soft Matter*, 2008, **4**, 2323–2330.
37 L. Deng, X. Trepat, J. P. Butler, E. Millet, K. G. Morgan, D. A. Weitz and J. J. Fredberg, *Nat. Mater.*, 2006, **5**, 636–640.
38 N. Rosenblatt, A. M. Alencar, A. Majumdar, B. Suki and D. Stamenovic, *Phys. Rev. Lett.*, 2006, **97**, 168101.
39 M. L. Gardel, J. H. Shin, F. C. MacKintosh, L. Mahadevan, P. A. Matsudaira and D. A. Weitz, *Phys. Rev. Lett.*, 2004, **93**, 188102.
40 C. P. Broedersz, C. Storm and F. C. MacKintosh, *Phys. Rev. Lett.*, 2008, **101**, 118103.
41 M. L. Gardel, F. Nakamura, J. H. Hartwig, J. C. Crocker, T. P. Stossel and D. A. Weitz, *Proc. Natl. Acad. Sci. U. S. A.*, 2006, **103**, 1762–1767.
42 G. H. Koenderink, Z. Dogic, F. Nakamura, P. M. Bendix, F. C. MacKintosh, J. H. Hartwig, T. P. Stossel and D. A. Weitz, *Proc. Natl. Acad. Sci. U. S. A.*, 2009, **106**, 15192–15197.
43 K. E. Kasza, F. Nakamura, S. Hu, P. Kollmannsberger, N. Bonakdar, B. Fabry, T. P. Stossel, N. Wang and D. A. Weitz, *Biophys. J.*, 2009, **96**, 4326–4335.
44 A. F. Huxley, *Prog. Biophys. Biophys. Chem.*, 1957, **7**, 255–318.
45 A. F. Huxley and R. M. Simmons, *Nature*, 1971, **233**, 533–538.
46 P. Fernandez and A. Ott, *Phys. Rev. Lett.*, 2008, **100**, 238102.
47 J. J. Fredberg, K. A. Jones, M. Nathan, S. Raboudi, Y. S. Prakash, S. A. Shore, J. P. Butler and G. C. Sieck, *J. Appl. Physiol.*, 1996, **81**, 2703–2712.
48 B. Guo and W. H. Guilford, *Proc. Natl. Acad. Sci. U. S. A.*, 2006, **103**, 9844–9849.
49 S. M. Mijailovich, J. P. Butler and J. J. Fredberg, *Biophys. J.*, 2000, **79**, 2667–2681.
50 P. Kollmannsberger and B. Fabry, *Soft Matter*, 2009, **5**, 1771–1774.
51 D. E. Discher, P. Janmey and Y. L. Wang, *Science*, 2005, **310**, 1139–1143.
52 U. Schwarz, *Soft Matter*, 2007, **3**, 263–266.
53 C. T. Mierke, P. Kollmannsberger, D. Paranhos-Zitterbart, J. Smith, B. Fabry and W. H. Goldmann, *Biophys. J.*, 2008, **94**, 661–670.